Boron nitride neutron detector with the ability for detecting both thermal and fast neutrons

A. Tingsuwatit, A. Maity, (iD) S. J. Grenadier, (iD) J. Li, (iD) J. Y. Lin, (iD) and H. X. Jiang[a] (iD)

AFFILIATIONS

Department of Electrical and Computer Engineering, Texas Tech University, Lubbock, Texas 79409, USA

[a]Author to whom correspondence should be addressed: hx.jiang@ttu.edu

ABSTRACT

The detection of fast neutrons is regarded technically challenging because the interaction probability of fast neutron with matter is extremely low. Based on our recent development of hexagonal boron nitride (BN) semiconductor thermal neutron detectors with a record high efficiency of 59%, we report here the feasibility studies of BN detectors for detecting fast neutrons. A BN detector with a detection area of 2.1 cm^2 was fabricated from a 90 μm thick BN epilayer. In the presence of a bare Cf-252 source emitting fast neutrons ranging from 1 to 9 MeV, the detection efficiency was estimated to be about 0.1%. The measured mean free path of fast neutron in BN is about 7.6 cm. Together with the capability of BN for thermal neutron detection, the present results indicate that by incorporating BN with a large thickness, BN neutron detectors are expected to possess the unique capability of directly detecting thermal to fast neutrons as well as outstanding features resulting from the ultrawide bandgap of BN. The identification of a single material that is sensitive to both thermal and fast neutrons is valuable for the development of novel neutron detection technologies.

Published under an exclusive license by AIP Publishing. https://doi.org/10.1063/5.0093591

Effective neutron detection methods are one of the key technologies that support safe nuclear power generation based on either fusion or fission, including monitoring nuclear reactors and identifying nuclear fuels. More specifically, fast neutron detection technologies provide a critical means for monitoring the neutron fluxes from fissile and fusion power generation systems and to assure radiation safety to the public.[1–5] Neutron detectors are also needed in various other application fields, including application areas of nuclear security, nuclear waste management, neutron generators, neutron radiography and scattering, oil field exploration, and life search in space. In many application areas, efficient detection of neutrons or neutron sources requires instruments that can sensitively detect and characterize neutrons in a wide range of energies. However, the interaction probability of fast neutrons with energies above 1 MeV with matter is extremely low, yielding a typical capture cross section on the order of ∼1 Barn.[6–8] As such, the detection of fast neutrons is still regarded technically challenging. Many types of neutron detectors have been developed to detect thermal neutrons (25 meV) due to their relatively large nuclear reaction rates or capture cross sections with ^{3}He, ^{6}Li, and ^{10}B.[9–25]

Most fast neutron detectors in use typically employ a large volume of neutron conversion material such as a large high-density polyethylene (HDPE) sphere to first convert fast neutrons to thermal neutrons, and then a ^{3}He gas thermal neutron detector is used to detect the neutron signal. Because the cross section for thermal neutrons is more than three orders of magnitude higher than those of fast neutrons, the detection efficiency and count rate are, in fact, increased by utilizing this conversion process. The disadvantages of this type of fast neutron detectors include loss of neutron energy information, bulky, heavy, nonportable, fixed operation range, and not convenient to operator. The world is also experiencing a shortage of ^{3}He gas because the demand for ^{3}He has been dramatically increased over the last decade,[5] not to mention that ^{3}He gas itself is a by-product (or nuclear waste) from nuclear weapons production. Alternative detector technologies including liquid noble-gas sensors[26–28] and plastic scintillator materials[29–32] have been successfully developed and deployed for fission material detection.

Semiconductor neutron detector technology is less developed but considered the ideal candidate for low-mass, low-power, and harsh environment applications.[9–25,33–41] Most developed semiconductor thermal neutron detectors use a thin neutron conversion layer of ^{6}Li or ^{10}B.[9–22] The limitation of this approach is that the conversion layer itself prevents neutron reaction products from depositing all their energies in the semiconductor detector's sensitive volume, which limits the detection efficiency for thermal neutrons.[9–22] While ^{10}B and ^{6}Li filled micro-structured semiconductor neutron detectors (MSND)

have attained a detection efficiency for thermal neutrons of 30%,[14–16,25] this technology, however, is not suitable for fast neutron detection. Diamond is very useful for detecting 14.6 MeV neutrons by utilizing the $^{12}C(n,\alpha)^9Be$ reaction.[42–44] However, diamond does not respond to thermal neutrons. The most common approach employed by the scientific community to partially overcome this shortfall is again to coat diamond with a neutron conversion layer of ^6Li or ^{10}B[42,43] with known limitations already discussed above.[9–22] Other problems limiting widespread use of diamond detectors are their small dimensions and high costs. For monocrystalline diamond, a typical film is less than 1 cm² in area and 500 μm in thickness and costs over $1500. SiC has also been investigated for fast neutron detection.[45] Similar to diamond, SiC itself is not sensitive to thermal neutrons. Previous studies have also revealed the usefulness of GaN for α particle detection, suggesting that GaN could be a neutron detection material when coated with a thin neutron conversion layer.[46] As of today, a single semiconductor material that is sensitive to both thermal and fast neutrons has not yet been identified. The development of such solid-state detectors is expected to provide new functionalities that previously not possible.

Hexagonal boron nitride (h-BN or BN), a member of the III-nitride wide bandgap semiconductor family, has shown great promises for neutron detection.[33–41] The nuclear reaction between ^{10}B in BN and thermal neutrons follows $^{10}B + {}^1_0n \rightarrow {}^7Li$ (1.015 MeV) + α (1.777 MeV) with 6% probability and $^{10}B + {}^1_0n \rightarrow {}^7Li^*$ (0.840 MeV) + α (1.470 MeV) with 94% probability, which yields a large nuclear reaction capture cross section of 3480 Barns.[24] The density of ^{10}B atoms in 100% ^{10}B-enriched BN is $N(^{10}B) = 5.5 \times 10^{22}/cm^3$. This provides a macroscopic cross section for thermal neutrons of $\alpha = N\sigma = 5.5 \times 10^{22} \times 3.84 \times 10^{-21} = 211.2$ cm^{-1} and a mean free path of $\lambda = \alpha^{-1} = 47.3$ μm for thermal neutrons in 100% B-10 enriched BN. Based on this physics principle for thermal neutron detection, we have recently realized epitaxial growth of thick BN films by metal organic chemical vapor deposition (MOCVD).[36–41] Thermal neutron detectors incorporating a BN epilayer of about 100 μm in thickness have demonstrated a record high detection efficiency (59%) and sensitivity among solid-state neutron detectors.[39] Moreover, BN detectors possess

all the outstanding features of ultrawide bandgap semiconductor devices with abilities to operate in extreme conditions.[40] In this work, we report the demonstration of the detection of fast neutrons (with energies in the range of 1–9 MeV) by a BN semiconductor detector.

The hexagonal BN epilayer used for the neutron detector fabrication is very similar to those described in previous works.[38–41] However, because of the extremely low interaction probability of fast neutron with matter, it is advantageous for the feasibility demonstration to fabricate a BN detector with a larger detection area. Briefly, the ^{10}B enriched (99.9%) hexagonal BN was grown by MOCVD on the c-plane sapphire substrate at a temperature of ∼1500 °C. A freestanding BN wafer of 4-in. in diameter was obtained via self-separation during cooling down after epi-growth, as depicted in Fig. 1(a), owing to the layer structured BN having a different thermal expansion coefficient than sapphire substrate. The freestanding wafer was then cut into strips of ∼1.4 mm in width and ∼2 cm in length via laser dicing. A highly resistive adhesive material (polyimide) was used to mount the detector strips on an insulating sub-mount (sapphire). Metal contacts consisting of a bi-layer of Ni (100 nm)/Au (40 nm) were deposited on the two edges of each BN strip using e-beam evaporation via a mask. Wire bonding was then performed to electrically connect the detector strips in parallel via the bonding pads of a semiconductor device package to form a detector with a total detection area of about 2.1 cm², as shown in Fig. 1(b), which is two times larger than our previously reported 1 cm² BN thermal detector.[39] A schematic showing a more detailed scheme of combining multiple detector strips can be found elsewhere.[39] The BN neutron detector architecture has been evolved from vertical thin film planar type[36,37] to lateral detector strips.[38–40] The strip detector geometry takes the advantage of the outstanding lateral transport properties of hexagonal BN[41] to support a high charge collection efficiency under a moderate bais voltage as well as to reduce the device capacitance by more than 230 times compared to a planar detector of the same detection area. The dark current–voltage charateristic of this detector is shown in Fig. 1(c), which reveals a room temperature resistivity of >10^{13} Ω cm. A bare Californium-252 (Cf-252) source (without the use of HDPE moderator) was
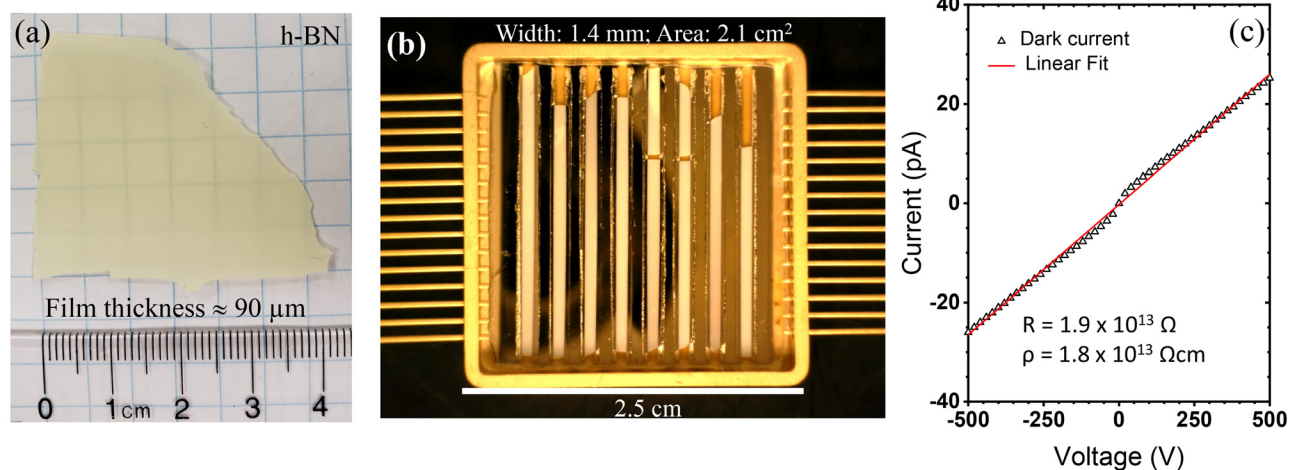
FIG. 1. Optical images of (a) a 90 μm thick freestanding hexagonal BN ¼-wafer and (b) a neutron detector fabricated from this BN freestanding wafer by combining multiple detector strips of ∼1.4 mm in width and ∼2 cm in length, providing a total detection area of ∼2.1 cm². (c) Current–voltage characteristic of this detector measured in the dark.

employed as a fast neutron source, which covers the neutron energy range from 1 to 9 MeV.[47]

In utilizing BN for fast neutron detection, the physics principle is based on charge carrier generation via recoil B and N ions upon elastic scattering by incoming fast neutrons and the subsequent collection of these charge carriers. The dominant elastic scattering cross sections of fast neutrons in the energy range between 0.5 and 20 MeV for ^{10}B, ^{11}B, and ^{14}N are around 1.3 Barns on average.[6–8] Using this cross section value and the B and N atomic densities in hexagonal BN of [N(B) = N(^{14}N) = 5.5×10^{22}/cm^3], the macroscopic cross section for fast neutrons in BN can, thus, be estimated as

$$\alpha = N\sigma = 5.5 \times 10^{22} \times 2 \times 1.3 \times 10^{-24} = 0.143 \, \text{cm}^{-1}, \quad (1)$$

which yields a mean free path of

$$\lambda = \alpha^{-1} = 7 \, \text{cm}. \quad (2)$$

To verify this calculated mean free path of fast neutrons in BN shown in Eq. (2), we have measured the transmission of fast neutrons in pyrolytic BN films. Pyrolytic BN films have a similar structural property as hexagonal BN semiconductors, except that they do not possess the necessary electronic properties to support the collection of neutron-generated charge carriers as the BN semiconductors do. Thus, the results of fast neutron transmission measured in pyrolytic BN represent those in BN semiconductors. Figure 2(a) is a schematic setup for monitoring fast neutrons from a bare Cf-252 source (without the use of HDPE moderator) transmitting through pyrolytic BN films. The relative fast neutron fluxes (T) passing through pyrolytic BN films of different thicknesses (d) were then recorded using the BN neutron detector shown in Fig. 1(b). The measured T is shown in Fig. 2(b) and follows the relation of

$$T \sim e^{-d/\lambda}, \quad (3)$$

where λ is the mean free path of fast neutrons in BN. The fitting between the measured data and Eq. (3) yields a value of $\lambda \approx 7.6$ cm,

which agrees well with the expected value of 7 cm calculated from the cross section of fast neutrons and atomic density of B and N atoms in hexagonal BN semiconductors of Eq. (2). Note that the measured mean free path of $\lambda = 7.6$ cm for fast neutrons is (a) averaged over the energy range of Cf-252 source, which covers from 1 to 9 MeV; (b) averaged over B-10, B-11, and N-14 atoms; (c) averaged over different scattering angles of elastic scattering between incoming fast neutrons and B and N atoms; and (d) including neutron absorption, inelastic scattering, and elastic scattering processes, whereas elastic scattering is the dominant process in this energy range.

Based on the experimental results of Fig. 2, the layer thickness (d) dependence of the intrinsic efficiency of the BN detector for fast neutrons in the energy range between 1 and 9 MeV can be estimated by using the following equation:

$$\eta_i(d) = 1 - e^{-d/\lambda}. \quad (4)$$

Equation (4) is plotted in Fig. 3, which establishes that a thickness of several centimeters is required to obtain a highly efficient BN detector for detecting fast neutrons. In the plot, $\lambda = 7.6$ cm is used based on experimental measurement results of Fig. 2. To demonstrate the feasibility of BN detectors for fast neutrons detection, the fabricated 2.1 cm^2 BN detector shown in Fig. 1(b) was used to directly detect fast neutrons emitted from a bare Cf-252 source (without a HDPE moderator). Figure 4 shows the pulsed height spectra obtained with and without the Cf-252 neutron source under a bias voltage of 300 V. The average counts acquired by the detector was 1937 over a 15-min counting time with the BN detector placed at 3 cm from the bare Cf-252 neutron source. Based on the known neutron flux at 3 cm from the bare Cf-252 neutron source and the measured count rate, a detection efficiency for fast neutrons from the ^{252}Cf source is estimated to be nearly 0.1% for a 90 μm thick BN detector. This measured result is within the expected intrinsic detection efficiency of $\eta_i \sim 0.12\%$ deduced from Eq. (4), considering the overall detection efficiency (η) is determined by both the intrinsic efficiency, $\eta_i(d)$, and charge
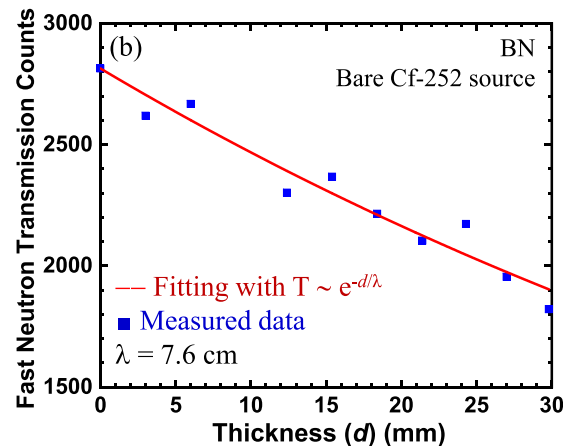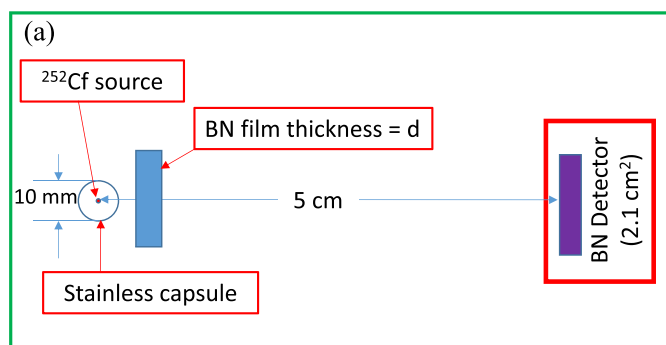
FIG. 2. (a) Schematic setup for measuring fast neutron transmission in BN from a bare Californium-252 (Cf-252) source. Pyrolytic BN films are used in-lieu-of BN, and the relative neutron fluxes passing through pyrolytic BN films of varying thicknesses (d) were recorded using the BN semiconductor neutron detector shown in Fig. 1(b). Pyrolytic BN films have a similar crystalline structural property as hexagonal BN except that they do not possess the necessary electronic properties to support the collection of neutron-generated charge carriers as the BN semiconductors do. (b) Relative fast neutron transmission (T) as a function of BN layer thickness (d). Dots represent experimental data, and solid curve represents a fit with Eq. (3).
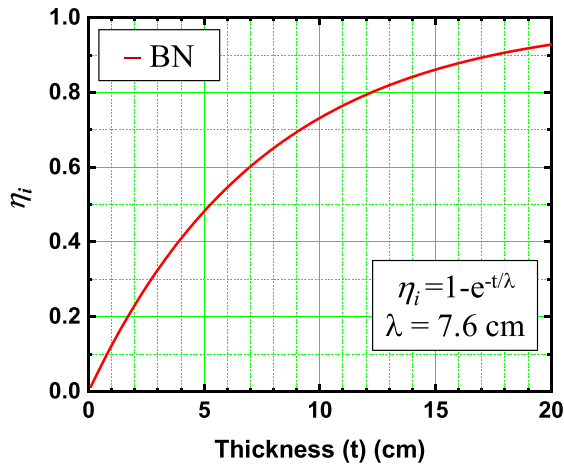
FIG. 3. Plot of Eq. (4)—the layer thickness dependence of the intrinsic efficiency (η_i) of BN detectors for fast neutrons.

collection efficiency (η_c), $\eta = \eta_i(d) \cdot \eta_c$, whereas η_c is expected to be less than 100%.

It is useful to point out that the detection efficiencies of BN detectors for fast neutrons are comparable regardless of whether they are constructed from B-10 enriched BN or from natural BN (where the element B exists as two main isotopes, ^{10}B and ^{11}B, in a natural abundance of approximately 20% and 80%, respectively) because the elastic scattering cross sections of B-10 and B-11 in the neutron energy range of 1–10 MeV are very comparable. The mean free path of thermal neutrons in natural BN is 237 μm. With further development, once BN films with a thickness exceeding 237 μm are realized, natural BN detectors are expected to provide the ability for directly detecting thermal to fast neutrons with a good efficiency. It is also important to note that BN detectors exhibit no response to gamma photons when directly exposed to a Caesium-137 source. This is because BN is composed of low atomic number elements.[36,39] However, Caesium-137 only has a single energy near 662 keV. For potential applications in nuclear reactor monitoring, it will be desirable to test the sensitivities
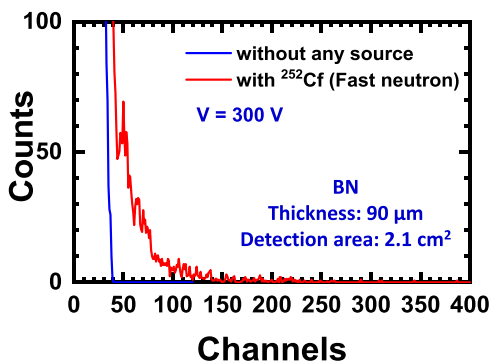
of BN detectors to low energy (tens to hundreds of keV) gamma photons.

While the highest interaction probability of fast neutron (above 1 MeV) with matter is via elastic scattering, the BN neutron detector demonstrated here is sensitive to both thermal and fast neutrons via nuclear reactions or recoil interactions. The detection of thermal neutrons by BN semiconductor detectors has already been demonstrated.[33–41] For fast neutron detection, after elastic scattering of fast neutrons with B or N atoms, the energy transferred from fast neutrons to recoil B or N ions will generate charge carriers. The collection of these charge carriers signifies the detection of fast neutrons as well as the energy of the recoil atoms, E_R, as described by

$$E_R = \left[4A/(1+A)^2\right](\cos^2 \theta_s) E_N, \quad (5)$$

where A is the atomic weight, and A = 10 for B-10 atoms, A = 11 for B-11 atoms, and A = 14 for N-14 atoms in BN. θ_s denotes the scattering angle and E_N the neutron energy. The recoil energy E_R decreases with an increase in the atomic weight. Since both boron and nitrogen atoms possess lowest atomic weight among all semiconductors, Eq. (5) reveals an important advantage of BN as a fast neutron detection material. A larger E_R value naturally translates to a larger number of charge carrier generation in BN and so a higher detection efficiency. The total number of free electrons (N_e) and holes (N_h), where $N_e = N_h$, generated from recoil energy E_R can be written as

$$N_e = N_h = E_R/3E_g, \quad (6)$$

where E_g is the energy bandgap of BN (≈ 6 eV). Guided by the result shown in Fig. 3 and Eq. (4), the required thickness of BN for attaining a practical detection efficiency for fast neutrons is several centimeters (cm). However, currently, it is not feasible to grow hexagonal BN epilayers with a few cm in thickness. Even if one can grow BN films with a few cm in thickness, it is impractical to supply the electric field on the order of 10^3 to 10^4 V/cm needed for charge collection. However, it is feasible to construct a stacked BN detector to provide an effective large thickness and area to provide a practical detection efficiency and sensitive for fast neutrons at a moderated bias voltage. It is worth mentioning that the energy transferred to the recoiled nucleus for the large scattering angle collisions may be below the threshold of detectable signals. As such, Eq. (4) represents an up limit theoretical efficiency for a thickness of d. An estimation of the expected detection efficiency and the energy threshold of the detector based on Monte Carlo simulation will be very valuable to guide the development of BN neutron detectors.

In the absence of any radiation, the variation of BN detector performance with time can be neglected because of the inherent stability of BN material itself in the air. Under neutron irradiation, B and N atoms will be displaced after each elastic scattering, a process that ends up generating two defects: one vacancy and one interstitial in BN. If a total count of 10^3 is needed to confirm a detection signal (the number of defects generated from each detection will be $\sim 10^3$) and assuming our 2 cm^2 detector will have a thickness of 500 μm in the near future, the estimate density of defects created in the detector can be estimated to be $10^3/0.1$ cm$^3 = 10^4$ cm^{-3}. If we target for a maximum 10^8 detection cycles during the lifetime of the detector (corresponding to a maximum rate capability of 10^{11}), the total density of defects generated will be on the order of 10^{12} cm^{-3}, which is four orders lower than the level of a typical impurity concentration (of greater than 10^{16} cm^{-3})

FIG. 4. Pulse height spectra of the BN semiconductor detector shown in Fig. 1(b) in response to fast neutrons from a bare ^{252}Cf source without the use of a HDPE moderator, covering the energy range from 1 to 9 MeV (red curve) and in the presence without any source (blue curve), all measured at 300 V.

needed to have any effects on the conductivity (or leakage current) of a semiconductor detector. Therefore, elastic scattering between fast neutrons and B and N atoms will not create a sufficient defect density, which otherwise would affect the performance of BN neutron detectors.

In summary, the feasibility of BN semiconductor detectors for detecting fast neutrons has been demonstrated by utilizing a 90 μm thick BN detector in response to a bare Cf-252 source emitting fast neutrons ranging from 1 to 9 MeV. The measured mean free path of fast neutrons with energies ranging from 1 to 9 MeV in BN is about 7.6 cm, which is consistent with the value deduced from the dominant interaction mechanism of elastic scattering and the atomic density of B or N atoms in BN. The present results together with our prior demonstrated results of BN thermal neutron detectors[29–34] suggest that by incorporating films with a sufficient thickness, it is feasible to realize high efficiency BN detectors, which are capable to directly detect both thermal and fast neutrons. With other outstanding features of an ultra-wide bandgap semiconductor, the development of BN semiconductor neutron detectors has the potential to replace ^{3}He gas tube-based detectors currently deployed in various application areas.

AUTHOR DECLARATIONS
Conflict of Interest

The authors have no conflicts to disclose.

Author Contributions

A. Tingsuwatit: Investigation (equal); Validation (equal). **A. Maity:** Investigation (equal); Methodology (equal). **S. J. Grenadier:** Investigation (equal); Methodology (equal). **J. Li:** Investigation (equal); Methodology (equal); Supervision (equal). **J. Y. Lin:** Conceptualization (equal); Data curation (equal); Formal analysis (equal); Funding acquisition (equal); Investigation (equal); Methodology (equal); Project administration (equal); Resources (equal); Supervision (equal); Validation (equal); Visualization (equal); Writing – original draft (equal); Writing – review & editing (equal). **H. X. Jiang:** Conceptualization (equal); Data curation (equal); Formal analysis (equal); Funding acquisition (equal); Investigation (equal); Methodology (equal); Project administration (equal); Resources (equal); Supervision (equal); Validation (equal); Visualization (equal); Writing – original draft (equal); Writing – review & editing (equal).

DATA AVAILABILITY

The data that support the findings of this study are available within the article.

REFERENCES

[1]D. Reilly, N. Ensslin, H. Smith, and S. Kreiner, "Passive nondestructive assay of nuclear materials," Technical Report No. NUREG/CR-5550 LA-UR-90-732 (Los Alamos National Laboratory, 1991).

[2]R. C. Haight, "Fast-neutron detectors for nuclear physics experiments," in *2nd International Workshop on Fast Neutron Detectors and Applications*, November 6–11 (EIN GEDI, Israel, 2011).

[3]S. Kiss, S. Lipcsei, G. Házi, T. Parkó, I. Pós, and Z. Kálya, "New refueling neutron monitoring and reactivity measurement systems for Paks NPP," in *27th International Conference Nuclear Energy for Europe*, September 10–13 (NENE, 2018).

[4]B. M. van der Ende, L. Li, D. Godin, and B. Sur, Nat. Commun. **10**, 1959 (2019).

[5]R. L. Kouzes, "The 3He supply problem, April 2009; Pacific Northwest National Laboratory," Contract No. DE-AC05-76RL01830 (U.S. Department of Energy, Pacific Northwest National Laboratory).

[6]See https://www.nrc.gov/docs/ML1122/ML11229A705.pdf for Interactions of Neutrons with Matter.

[7]See https://www.osti.gov/servlets/purl/7329788 for Light element standard cross sections for ENDF/B.

[8]See https://www-nds.iaea.org/exfor/endf.htm for Evaluated Nuclear Data File.

[9]A. Rose, Nucl. Instrum. Methods **52**, 166 (1967).

[10]R. J. Nikolic, C. L. Cheung, C. E. Reinhardt, and T. F. Wang, "Future of semiconductor based thermal neutron detectors," *Nanotech, Boston, MA, May 07-11 2006* (2006), available at https://www.osti.gov/biblio/893992.

[11]D. S. McGregor, R. T. Klann, H. K. Gersch, and Y. H. Yang, Nucl. Instrum. Methods Phys. Res., Sect. A **466**, 126 (2001).

[12]H. K. Gersch, D. S. McGregor, and P. A. Simpson, Nucl. Instrum. Methods Phys. Res., Sect. A **489**, 85 (2002).

[13]N. LiCausi, J. Dingley, Y. Danon, J. Q. Lu, and I. B. Bhat, Proc. SPIE **7079**, 707908 (2008).

[14]R. J. Nikolic, A. M. Conway, C. E. Reinhardt, R. T. Graff, T. F. Wang, N. Deo, and C. L. Cheung, Appl. Phys. Lett. **93**, 133502 (2008).

[15]R. J. Nikolic, C. L. Cheung, C. E. Reinhardt, and T. F. Wang, Proc. SPIE **6013**, 601305 (2005).

[16]A. M. Conway, T. F. Wang, N. Deo, C. L. Cheung, and R. J. Nikolic, IEEE Trans. Nucl. Sci. **56**, 2802 (2009).

[17]R. Dahal, K. C. Huang, J. Clinton, N. LiCausi, J.-Q. Lu, Y. Danon, and I. Bhat, Appl. Phys. Lett. **100**, 243507 (2012).

[18]F. Wald and J. Bulitt, "Semiconductor neutron detectors," Report No. 771526/1GA (1973).

[19]K. P. Ananthanarayanan, P. J. Gielisse, and A. Choudry, Nucl. Instrum. Methods **118**, 45 (1974).

[20]P. Lunca-Popa, J. I. Brand, S. Balaz, L. G. Rosa, N. M. Boag, M. Bai, B. W. Robertson, and P. A. Dowben, J. Phys. D **38**, 1248 (2005).

[21]S. Adenwalla, P. Welsch, A. Harken, J. I. Brand, A. Sezer, and B. W. Robertson, Appl. Phys. Lett. **79**, 4357 (2001).

[22]K. Osberg, N. Schemm, S. Balkir, J. O. Brand, M. S. Hallbeck, P. A. Dowben, and M. W. Hoffman, IEEE Sensor J. **6**, 1531 (2006).

[23]F. P. Doty, "Boron nitride solid-state neutron detector," Report No. SAND2003-8796 (Sandia National Laboratories, Livermore, 2003).

[24]G. F. Knoll, "Radiation Detection and Measurement," 4th ed. (John Wiley & Sons, 2010).

[25]D. S. McGregor, S. L. Bellinger, J. C. Boyington, Y. Cheng, and R. G. Fronk, see https://newprairiepress.org/cgi/viewcontent.cgi?article=1009&context=asemot for "Symposium on Advanced Sensors and Modeling Techniques for Nuclear Reactor Safety"

[26]J. Kwong, T. Gozani, M. J. King, S. Kane, C. Gary, M. I. Firestone, J. A. Nikkel, and D. N. McKinsey, IEEE Trans. Nucl. Sci. **60**, 652 (2013).

[27]J. A. Nikkel, T. Gozani, C. Brown, J. Kwong, D. N. McKinsey, Y. Shin, S. Kane, C. Garyc, and M. Firestone, J. Instrum. **7**, C03007 (2012).

[28]R. Jebali, J. Scherzinger, J. R. M. Annand, R. Chandra, G. Davatz, K. G. Fissum, H. Friederich, U. Gendotti, R. Hall-Wilton, E. Håkansson, K. Kanaki, M. Lundin, D. Murer, B. Nilsson, A. Rosborg, and H. Svensson, Nucl. Instrum. Methods Phys. Res., Sect. A **794**, 102 (2015).

[29]Y. I. Chernukhin, A. A. Yudov, and S. I. Streltsov, Nucl. Energy Technol. **1**, 130 (2015).

[30]M. J. Cieślak, K. A. A. Gamage, and R. Glover, Crystals **9**, 480 (2019).

[31]C. Frangville, A. Grabowski, J. Dumazert, E. Montbarbon, C. Lynde, R. Coulon, A. Venerosy, G. H. Bertrand, and M. Hamel, Nucl. Instrum. Methods Phys. Res., Sect. A **942**, 162370 (2019).

[32]N. Zaitseva, A. Glenn, A. Mabe, L. Carman, and S. Payne, Int. J. Mod. Phys. **50**, 2060003 (2020).

[33]H. X. Jiang, J. Y. Lin, J. Li, A. Maity, and S. J. Grenadier, "Solid-state neutron detector," U.S. patent 10,714,651 B2 and U.S. patent 11,195,968 B2.

[34]A. Maity, S. J. Grenadier, J. Li, J. Y. Lin, and H. X. Jiang, Prog. Quantum. Electron. **76**, 100302 (2021).

[35]S. J. Grenadier, A. Maity, J. Li, J. Y. Lin, and H. X. Jiang, "Chapter 12— Electrical transport properties of hexagonal boron nitride epilayers," *Semiconductors and Semimetals*, edited by Y. Zhao and Z. Mi (Elsevier, 2021), Vol. 107, pp. 393–454.

[36]A. Maity, T. C. Doan, J. Li, J. Y. Lin, and H. X. Jiang, Appl. Phys. Lett. **109**, 072101 (2016).

[37]A. Maity, S. J. Grenadier, J. Li, J. Y. Lin, and H. X. Jiang, Appl. Phys. Lett. **111**, 033507 (2017); J. Appl. Phys. **123**, 044501 (2018).

[38]A. Maity, S. J. Grenadier, J. Li, J. Y. Lin, and H. X. Jiang, Appl. Phys. Lett. **114**, 222102 (2019).

[39]A. Maity, S. J. Grenadier, J. Li, J. Y. Lin, and H. X. Jiang, Appl. Phys. Lett. **116**, 142102 (2020).

[40]J. Li, A. Maity, S. J. Grenadier, J. Y. Lin, and H. X. Jiang, Appl. Phys. Lett. **118**, 092102 (2021).

[41]S. J. Grenadier, A. Maity, J. Li, J. Y. Lin, and H. X. Jiang, Appl. Phys. Lett. **115**, 072108 (2019).

[42]M. Angelone, in Proceedings of a Technical Meeting, Modern Neutron Detection, 2020, available at https://www-pub.iaea.org/MTCD/Publications/PDF/TE-1935_web.pdf.

[43]S. Almaviva, M. Marinelli, E. Milani, G. Prestopino, 1 A. Tucciarone, C. Verona, G. Verona-Rinati, M. Angelone, D. Lattanzi, M. Pillon, R. M. Montereali, and M. A. Vincenti, J. Appl. Phys. **103**, 054501 (2008).

[44]P. Kavrigin, E. Griesmayer, F. Belloni, A. J. M. Plompen, P. Schillebeeckx, and C. Weiss, Eur. Phys. J. A **52**, 179 (2016).

[45]L. Wang, J. Jarrell, S. Xue, C. Tan, T. Blue, and L. R. Cao, Nucl. Instrum. Methods Phys. Res., Sect. A **888**, 126 (2018).

[46]J. Wang, P. Mulligan, L. Brillson, and L. R. Cao, Appl. Phys. Rev. **2**, 031102 (2015).

[47]S. T. Park, J. Radioanal. Nucl. Chem. **256**, 163 (2003).